AIP | Applied Physics Letters

Effect of liquid spreading due to nano/microstructures on the critical heat flux during pool boiling

Ho Seon Ahn, Hang Jin Jo, Soon Ho Kang, and Moo Hwan Kim

Citation: Applied Physics Letters **98**, 071908 (2011); doi: 10.1063/1.3555430
View online: http://dx.doi.org/10.1063/1.3555430
View Table of Contents: http://scitation.aip.org/content/aip/journal/apl/98/7?ver=pdfcov
Published by the AIP Publishing

Articles you may be interested in

Enhancement of critical heat flux in pool boiling using atomic layer deposition of alumina
Appl. Phys. Lett. **100**, 053120 (2012); 10.1063/1.3681943

Effects of nanoparticle layering on nanofluid and base fluid pool boiling heat transfer from a horizontal surface under atmospheric pressure
J. Appl. Phys. **107**, 114302 (2010); 10.1063/1.3342584

Effects of nanoparticle deposition on surface wettability influencing boiling heat transfer in nanofluids
Appl. Phys. Lett. **89**, 153107 (2006); 10.1063/1.2360892

On the role of structural disjoining pressure and contact line pinning in critical heat flux enhancement during boiling of nanofluids
Appl. Phys. Lett. **89**, 044106 (2006); 10.1063/1.2222283

Effect of nanoparticles on critical heat flux of water in pool boiling heat transfer
Appl. Phys. Lett. **83**, 3374 (2003); 10.1063/1.1619206

Want to publish your paper in the
#1 MOST CITED journal in applied physics?
With *Applied Physics Letters*, you can.

AIP | Applied Physics Letters

THERE'S POWER IN NUMBERS. Reach the world with AIP Publishing.

This article is copyrighted as indicated in the article. Reuse of AIP content is subject to the terms at: http://scitation.aip.org/termsconditions. Downloaded to IP: 141.223.173.110 On: Wed, 22 Apr 2015 06:45:04

Effect of liquid spreading due to nano/microstructures on the critical heat flux during pool boiling

Ho Seon Ahn,[1] Hang Jin Jo,[1] Soon Ho Kang,[1] and Moo Hwan Kim[2,a)]
[1]*Department of Mechanical Engineering, POSTECH, Pohang, 790-784, Republic of Korea*
[2]*Division of Advanced Nuclear Engineering, POSTECH, Pohang, 790-784, Republic of Korea*

(Received 31 October 2010; accepted 26 January 2011; published online 15 February 2011)

It is well known that nanoparticles deposited on a heating surface during nanofluid boiling can change the characteristics of the heating surface and increase the critical heat flux (CHF) dramatically. We considered a new approach to investigate the nanoparticle surface effect on CHF enhancement using surfaces modified with artificial micro/nanostructures similar to deposited nanoparticle structures. We examined the effect of the surface wettability and liquid spreading ability on the CHF. The results demonstrated that the CHF enhancement on the modified surfaces was a consequence of both the improved surface wettability and the liquid spreading ability of the artificial micro/nanostructures. © *2011 American Institute of Physics*. [doi:10.1063/1.3555430]

It is widely recognized that when a nanofluids is boiled on a heating surface, the deposited nanoparticles enhance the critical heat flux (CHF) by changing the surface wettability characteristics.[1–3] Kim *et al.*[4] performed a pool boiling experiment using pure water on surfaces with deposited nanoparticles that were produced while pool boiling water-TiO_2 and water-Al_2O_3 nanofluids. This clearly shows that the nanoparticles deposited on the heating surface are the main cause of the CHF enhancement. Kim *et al.*[5] proposed a simple model consisting of a nanoparticle absorption layer to describe how nanoparticles change the surface wettability. Kim and Kim[6] postulated that the wettability and capillarity of a heating surface could influence the CHF enhancement. They explained that the CHF increases the liquid supply on the heating surface due to the capillarity of the nanoparticle absorption layer. However, it was only possible to measure the capillarity of a heater with deposited nanoparticles using a one-directional thin-wire heater. In addition, nanoparticle on heating surface has many problems to adjust the application, because of its robustness (the detached problem of nanoparticles under flow boiling).[7]

Dhir[8] made wettable heater surfaces using thermal oxidation and concluded that the CHF increased with the wettability of the heater surface. Recently, Ahn *et al.*[9] used an experimental approach to enhance the CHF of an artificial surface similar to a nanoparticle deposition layer after pool boiling in a nanofluid. They used a plate heater surface made of zirconium alloy (zircaloy-4) for the pool boiling CHF experiment; this is the same material used in nuclear fuel rod cladding. Anodic oxidation was used to change the morphology and wettability of the heater surface. The CHF of the modified surface increased as the static contact angle decreased. The CHF increased significantly below a contact angle of 10°, disagreeing with the predictions of Kandlikar,[10] which include the effect of wettability on the CHF. Liquid spreading was observed on surfaces with contact angles less than 10°.

The objective of this study was to examine the relationship between the CHF enhancement in pool boiling and the changes in surface characteristics such as surface wettability and liquid spreading, which are closely related to the rewetting of a dry patch during boiling. The effect of liquid spreading on the CHF was investigated quantitatively through visualization of the dynamic motion of droplets on the modified (micro, nano, micro/nanostructured) surfaces. The CHF experiments on modified surfaces were conducted on plate heater (10 mm × 10 mm) using the conducted heating method.

An anodic oxidation process (HF 0.5%, 20 V) was used to prepare the test surfaces, which consisted of thermally heated zirconium-alloy plates .[9] Scanning electron microscopy (SEM) images showed that the test surfaces developed different structures as the anodic oxidation time increased but there was no change in the structures for oxidation times greater than 12–15 min [Fig. 1(a)]. To characterize the surface wettability, the apparent static/dynamic contact angles

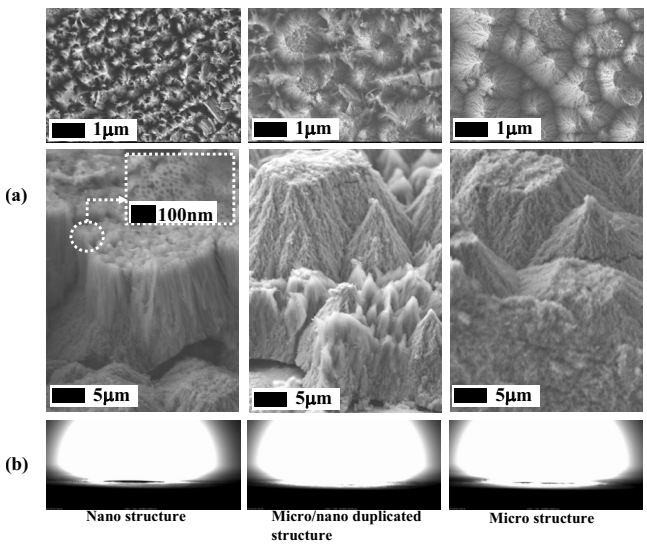

FIG. 1. Test surfaces promoting liquid spreading at a contact angle less than 10°. (a) SEM images and (b) apparent static contact angle. As the anodic oxidation time increases, surfaces develop nano, micro/nano, and microstructures in that order. Surfaces composed of nanostructures (or nanotubes) have near-complete wetting (2°–9.2°). Micro/nano and microsurfaces have perfect complete wetting (0°). Their CHF values could not explained by only wettability effect as Fig. 2.

a)Author to whom correspondence should be addressed. Electronic mail: mhkim@postech.ac.kr.

 © 2011 American Institute of Physics

This article is copyrighted as indicated in the article. Reuse of AIP content is subject to the terms at: http://scitation.aip.org/termsconditions. Downloaded to IP: 141.223.173.110 On: Wed, 22 Apr 2015 06:45:04

were measured using 1 μL water droplets placed on surfaces with micro, nano, and micro/nano structures they had an uncertainty of $\pm 1°$. The dynamic motion of a droplet on the test surfaces was captured using a high-speed camera.

Figure 2 shows the results of our CHF experiments, as well as Kandlikar's predictions,[10] which include the effect of surface wettability. The CHF of the micro, nano, and micro/nanostructured surfaces increased more than indicated by Kandlikar's predictions[10] below a contact angle of 10°. The micro/nanoduplicated structured surface had the maximum CHF in Fig. 2(c) and its spreading ability also could be observed as maximum, which there was just precursor line without the contact line of droplet. Figures 2(a) and 2(b) were the nanostructured surfaces and Fig. 2(d) was just microstructured surface (see Fig. 1). The liquid spreading was induced by the liquid suction of the absorption layer of the structures.[11–13] When a thin absorption layer exists beneath a growing bubble during boiling, liquid suction along the layer promotes hot-spot rewetting, thus, delaying the CHF.[6,9,13] However, it is very difficult to measure the amount of liquid suction or to estimate the effect of liquid spreading for a plate heater.

In this study, a simple model is proposed to determine the amount of absorbed liquid in micro, nano, and micro/nanostructured surfaces (these surfaces had the liquid spreading due to their absorbed layer) based on a dynamic droplet-motion analysis [Fig. 3(a)]. The water droplet (10 μL) was dropped at 23 °C air with on micro, nano, and micro/nanostructured surfaces which were used for the CHF experiments. Our main assumption is that droplets spreading in an absorption layer are spherical. Then $\Omega = 4/3\pi R_{\text{drop}}^3$ and $\Omega' = 1/4\pi R_{\text{curvature}}^3 \theta_D^4$, where Ω is the original droplet volume, Ω' is the remained (spreading) droplet volume (neglecting the O(6) of θ_D during Taylor's expansion), R_{drop} is the radius of the droplet, $R_{\text{curvature}}$ is the curvature of the spreading droplet on test surfaces, and θ_D is the dynamic contact angle. Because the test surfaces contains an absorption layer for the micro, nano, and micro/nanostructures, the original droplet volume (Ω) should be larger than the remained (spreading) droplet volume (Ω'). The amount of absorbed liquid ($\Phi = \Omega - \Omega'$) is defined as the volume difference between the original droplet and the spreading droplet. The amount change in liquid suction in the absorbed layer when the characteristics of surfaces change from dry to wet is as follows: $\dot{\Phi} = d\Phi/dt = d/dt(\Omega - \Omega') = d/dt(\Omega - 1/4\pi R_{\text{curvature}}^3 \theta_D^4)$. From this analytical equation, we can calculate the differential volume change in the amount of absorbed liquid (the absolute value of $d\Phi/dt$). Given that Ω is constant,

$$\frac{d\Phi}{dt} = \frac{1}{4}\pi R_{\text{curvature}}^2 \theta_D^3 \left(3\theta_D \frac{dR_{\text{curvature}}}{dt} + 4R_{\text{curvature}} \frac{d\theta_D}{dt}\right), \tag{1}$$

where $dR_{\text{curvature}}/dt$ is the differential value of the spreading droplet radius and $d\theta_D/dt$ is the differential value of the dynamic contact angle. Equation (1) seemed that the differential volume change in the amount of absorbed liquid was related with time. These values were determined from high-time-resolution (5000 frames/sec) visualization results using the spline circle fitting method and from measurements of the dynamic contact angle [see Fig. 3(a)]. Figure 3(b) shows the relations with the curvature of spreading droplet, the dynamic contact angle, and the time on microstructured surface, respectively. The curvature radius was represented as $R \sim X\Omega^m t^n$ where X, m, and n are empirical constants.[14] Figure 3(b) shows that the curvature radius ($R_{\text{curvature}}$) is the monotone increasing function of time ($n \sim 1$) in the available

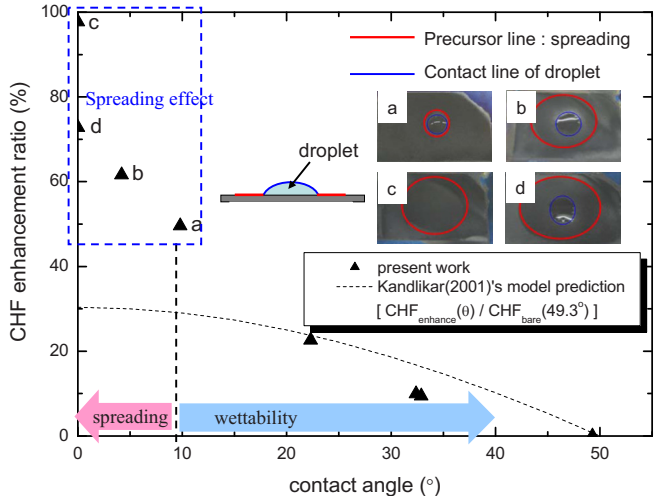

FIG. 2. (Color online) CHF experimental data and Kandlikar's prediction [CHF enhancement ratio: $[\text{CHF}_{\text{enhance}}(\theta_D)/\text{CHF}_{\text{bare}(49.3°)}]$]. At a contact angle less than 10°, the liquid spreading on a heating surface is the dominant CHF enhancement mechanism. (a) nanostructure, (b) nanostructure, (c) micro/nanostructure, and (d) microstructure.

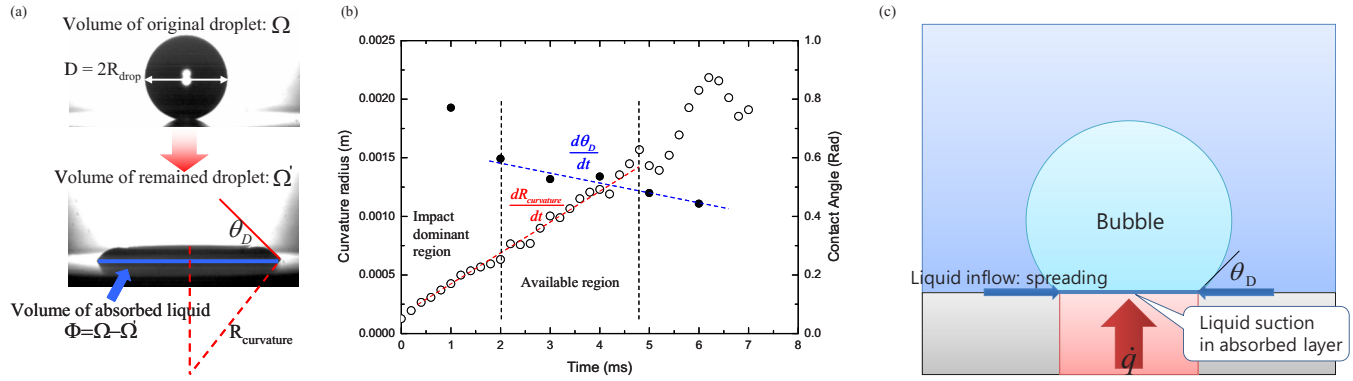

FIG. 3. (Color online) Liquid spreading model for the absorption layer. The difference between the volumes of the original and the remained (spreading) droplets is the volume of the liquid absorbed by the absorption layer. (a) Calculation concept of the absorbed liquid volume through the dynamic wetting test of liquid droplet. (b) The curvature radius ($R_{\text{curvature}}$) and the dynamic contact angle on microstructured surface. The available region consisted both advancing and spreading by precursor layer inside micro, nano, and micro/nanostructures (Ref. 15). (c) Schematic diagram of the CHF model including liquid spreading.

This article is copyrighted as indicated in the article. Reuse of AIP content is subject to the terms at: http://scitation.aip.org/termsconditions. Downloaded to IP: 141.223.173.110 On: Wed, 22 Apr 2015 06:45:04

region.[15] The available region (capillary invasion region) of the curvature radius and the dynamic contact angle in Fig. 3(b) was defined in previous research.[15] We decided the available region based on the dynamic wetting images which can be seemed like the liquid spreading by precursor layer inside structures. Since the dynamic contact angle (θ_D) is lower than 1 rad ($\theta_D < 1$), the third or fourth power values (θ_D^3 or θ_D^4) in Eq. (1) are nearly constant in the available region.[15] Therefore, the values of $R_{\text{curvature}}$, dR/dt, $d\theta_D/dt$, and θ_D could be time-averaged to calculate the volume change in the absorbed liquid ($d\Phi/dt$), then they could be expressed as $\overline{R_{\text{curvature}}}$, $\overline{dR/dt}$, $\overline{d\theta_D/dt}$, and $\overline{\theta_D}$.

Figure 3(c) shows the concept of a liquid suction layer beneath a bubble mushroom. Liquid spreading occurred on the dried surface in all directions along the triple line (macroscopic view) of the bubble, heater, and liquid. Finally, the attainable heat flux, including the effect of liquid spreading, was calculated using the measured droplet-spreading dynamics as $q''_{\text{spreading\_liquid\_supplying}} = (d\Phi/dt)\rho_l h_{fg}/A_{\text{heating\_surface}}$, where ρ_l is the liquid density and h_{fg} is the latent heat. The CHF enhancement on the test surfaces was influenced by both the wettability and the liquid spreading, as shown in Fig. 2. Therefore, the final estimated CHF was

$$
\begin{aligned}
q''_{\text{CHF}} = q''_{\text{CHF\_Kandlikar}} + q''_{\text{spreading\_liquid\_supplying}} = S \\
\times h_{fg}\rho_g^{1/2}\left(\frac{1+\cos\theta_D}{16}\right)\left[\frac{2}{\pi}+\frac{\pi}{4}(1\right. \\
\left.+\cos\theta_D)\cos\phi\right]^{1/2}[\sigma g(\rho_l-\rho_g)]^{1/4} \\
+\frac{1}{4}\pi(k\overline{R_{\text{curvature}}})^2\overline{\theta_D^3}\left(3\overline{\theta_D}\overline{\frac{dR_{\text{curvature}}}{dt}}\right. \\
\left.+4k\overline{R_{\text{curvature}}}\overline{\frac{d\theta_D}{dt}}\right)\rho_l h_{fg}/A_{\text{heating\_surface}}, \qquad (2)
\end{aligned}
$$

where ϕ, σ, ρ_g, and $A_{\text{heating\_surface}}$ are the inclined angle of the heater, surface tension, vapor density, and the heater's area, respectively. Since the curvature radius ($\overline{R_{\text{curvature}}}$) is not the exact value but time-averaged value approximately in available region, because the time-averaged value of the curvature radius cannot represent it in real boiling situation, the effective parameter (k) was multiplied by the curvature value to fit the experimental CHF results using Eq. (2). ($R_{\text{curvature}}$ was replaced by $kR_{\text{curvature}}$ to fit the CHF results, $k=0.6$) Figure 4 shows that the estimated heat flux based on the liquid spreading and wettability was corresponded well with the experimental CHF increase above the CHF value that was obtained considering the wettability enhancement of Kandlikar's predictions[10] and based on the measured contact angle. As the CHF value of the bare surface does not agree with Kandlikar's prediction due to the heater size effect, Kandlikar's bare surface CHF prediction (49.3°) was multiplied by a constant factor ($S=0.823$) to fit the experimental data. Kandlikar's CHF model has a heater-size limitation and is based on a circular heater with a diameter of 10 mm. The heat flux gain of liquid spreading below a contact angle of 10° was calculated and also plotted using Eq. (2) in Fig. 4.

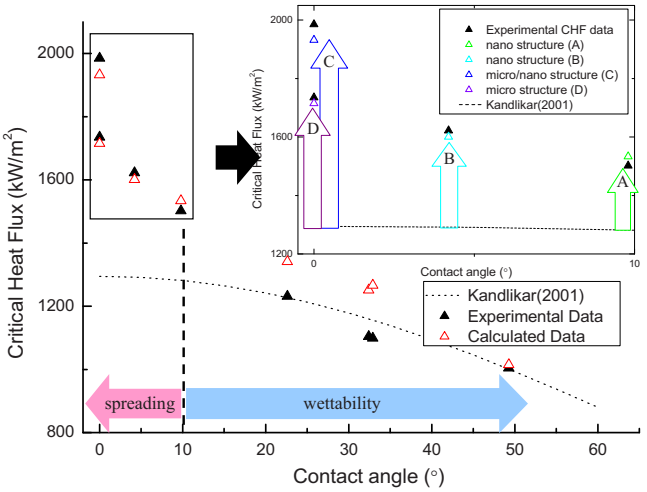

FIG. 4. (Color online) CHF values of experimental data and the developed prediction based on Eq. (2). The heat fluxes due to liquid spreading are: (a) nanostructure: 177 kW/m^2, (b) nanostructure: 251 kW/m^2, (c) micro/nanostructure: 560 kW/m^2, and (d) microstructure: 343 kW/m^2. The micro/nanoduplicated structure has the highest CHF value due to its having the most liquid spreading.

The results demonstrated that a simple model of the dynamic droplet motion on dry nano, micro, and nano/microstructured surfaces could represent quantitatively the heat flux gain due to the liquid spreading. We can, therefore, conclude that the significant CHF enhancement on heating surfaces with liquid spreading during pool boiling is a consequence not only of the increased surface wettability, but also of the improved liquid spreading due to the nano, micro, and nano/microstructures. The nano/microstructured surface had the greatest liquid spreading ability and the maximum CHF. The amount of liquid suction due to liquid spreading was obtained by developing a simple model and its effect on CHF enhancement was verified by experimental data.

This research was supported by WCU (World Class University) program through the National Research Foundation of Korea funded by the Ministry of Education, Science, and Technology (Grant No. R31-30005).

[1]J. A. Eastman, S. U. S. Choi, S. Li, W. Yu, and L. J. Thompson, Appl. Phys. Lett. **78**, 718 (2001).
[2]S. M. You, J. H. Kim, and K. H. Kim, Appl. Phys. Lett. **83**, 3374 (2003).
[3]P. Vassallo, R. Kumar, and S. D'Amico, Int. J. Heat Mass Transfer **47**, 407 (2004).
[4]H. D. Kim, J. B. Kim, and M. H. Kim, Int. J. Heat Mass Transfer **49**, 5070 (2006).
[5]S. J. Kim, I. C. Bang, J. Buongiorno, and L. W. Hu, Appl. Phys. Lett. **89**, 153107 (2006).
[6]H. D. Kim and M. H. Kim, Appl. Phys. Lett. **91**, 014104 (2007).
[7]H. S. Ahn, H. Kim, H. J. Jo, S. H. Kang, W. P. Chang, and M. H. Kim, Int. J. Multiphase Flow **36**, 375 (2010).
[8]V. K. Dhir, Annu. Rev. Fluid Mech. **30**, 365 (1998).
[9]H. S. Ahn, C. Lee, H. Kim, H. J. Jo, S. H. Kang, J. Kim, and M. H. Kim, Nucl. Eng. Des. **240**, 3350 (2010).
[10]S. G. Kandlikar, J. Heat Transfer **123**, 1071 (2001).
[11]Y. Chen, L. S. Melvin, S. Rodriguez, and M. M. Weislogel, Microelectron. Eng. **86**, 1317 (2009).
[12]C. Ishino, M. Reyssat, E. Reyssat, and D. Quere, EPL **79**, 56005 (2007).
[13]S. T. Kim, H. Kim, H. D. Kim, H. S. Ahn, H. J. Jo, J. Kim, and M. H. Kim, Exp. Therm. Fluid Sci. **34**, 487 (2010).
[14]J.-G. Fan and Y.-P. Zhao, Appl. Phys. Lett. **90**, 013102 (2007).
[15]J.-G. Fan, D. Dyer, G. Zhang, and Y.-P. Zhao, Nano Lett. **4**, 2133 (2004).

This article is copyrighted as indicated in the article. Reuse of AIP content is subject to the terms at: http://scitation.aip.org/termsconditions. Downloaded to IP: 141.223.173.110 On: Wed, 22 Apr 2015 06:45:04